Physical Modelling in Geotechnics

2D effect of static or rolling load on a granular platform above a soft soil reinforced by rigid inclusions

T. Dubreucq, L. Thorel, S. Lerat, A. Jagu & A. Néel
GERS-CG, Univ. Gustave Eiffel, IFSTTAR, F-44344 Bouguenais, France

ABSTRACT: The effect of static or rolling loads on a thin load transfer platform installed on a soft soil reinforced by rigid inclusions is investigated in a 2D geometry. The centrifuge model, scaled at 1/10th, consists of a sandy layer, an analog polystyrene soft soil and spaced vertical metal plates. A strongbox with a transparent face allows image analysis during loading. At a g-level of 10, this model was subjected to static vertical loading of a shallow foundation, and to mobile loading. Few round-trip cycles were carried out to simulate linear traffic. The roller mass can vary from test to test over the range of platform service loads up to the critical load measured statically.

Keywords: Soil improvement, rigid inclusions, load transfer platform, centrifuge, rolling load

1 INTRODUCTION

The improvement of soft soils with vertical rigid inclusions is now a widespread technique (e.g. ASIRI, Rigid Inclusion Ground Improvements, 2013). In the framework of the French National Research Programme ASIRI+ (Briançon et al., 2020; ASIRI+, 2021), launched in 2019, new research topics have been investigated, including the case of the rolling load.

One approach used is the centrifuge modelling. Here, the experimental work in macro-gravity concerns the 2D study of the behavior of thin load transfer platform (LTP) installed on a soft soil reinforced by rigid inclusions (RI) subjected to static loads or rolling loads induced by traffic on the platform (Fig. 1).

From the top to the bottom, the physical model consists of a sandy layer (the granular LTP) covered by a plastic film for rolling load case, an analog soft polystyrene soil (geofoam) and spaced vertical metal plates (to simulate RI) installed on a rigid substratum.

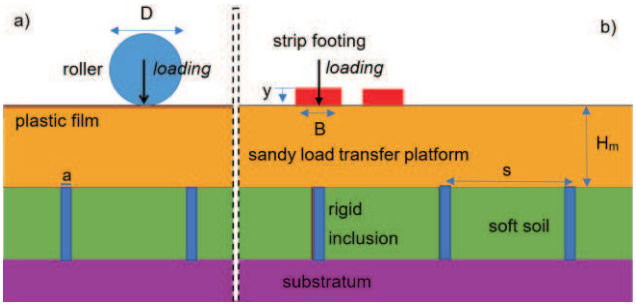

Fig. 1. 2D geometry of the physical model – a) roller in translation; b) static loading of a strip footing above a RI or between two RI.

2D geometry is a first step (Lukiantchuki et al., 2018) in the understanding of load transfer. Successively the 1/10th scale two-dimension static and rolling designs, and some first results will be presented. Each model is placed in a rigid strongbox with a transparent face, under an acceleration of 10×g, to visualize in the LTP the deformations and failure mechanisms under vertical static/cyclic loading. The strip footing width B takes 2 values, as well as H_m, height of the LTP ; the spacing s between RI and the width a of a RI are constant (Fig.1), the strip footing settlement in the center being y.

2 STATIC LOADS

2.1 Design of the 2D static model

In a first rigid container (54 cm long and 22 cm wide, Fig.2), two strip aluminum footings were used in turn: B equals to 3 and 6 cm with a length L = 18 cm. A ball joint ensures the foundation-actuator connection. The underside of the two strip footings has been roughened by sandblasting.

The acceleration of 10×g is applied to the base of the strip footing. The quasi static loading is vertical, centered and controlled in displacement at the speed of 0.5 mm/min for all the tests, by means of an electric actuator which is fixed to a reaction beam.

The LTP is a NE 34 Fontainebleau sand (Dano et al., 2022). Its thickness H_m is equal to 40 cm or 60 cm in prototype scale. The sand (d_{50} = 0.21mm) is moderately dense (I_d = 0.75).

© 2022 KOREAN GEOTECHNICAL SOCIETY (KGS), Seoul, Korea, ISBN 978-89-952197-7-5

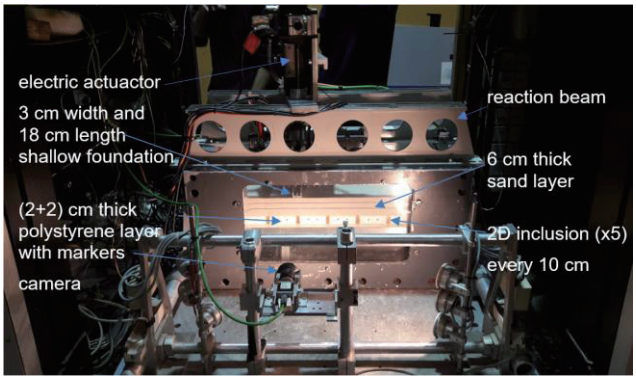

Fig. 2. The shallow foundation loading test behind the glass of the transparent-faced strongbox installed in the centrifuge basket.

It is implemented by air pluviation in the container to obtain a dry density of 1648 kg/m^3. Its friction angle is 32 degrees with zero effective cohesion.

The 2D RI located every s=10 cm consists of flat rigid aluminum plates, laid on a thick rigid aluminum plate to simulate substratum. Their rotation in the plane of the window is blocked at the back. The RI thickness is a=1 cm. The area of the inclusion over the area of the continuous mesh is thus $\alpha = 10\%$. The surface of these RI's heads has been also sandblasted to give them a normalized roughness $R_n=R_{max}/d_{50} = 0.46$ which implies an interface friction closed to concrete RI/sand friction.

The compressible soil is simulated with a 15.5 kg/m^3 expanded polystyrene (Th.38, Knauf©). Two superimposed 2 cm thick layers (40 cm in prototype scale, Fig.2) are arranged above the substratum. Compression is followed with mobile marker image analysis. With an almost zero Poisson's ratio, the polystyrene practically does not transmit horizontal pressure on the RI when it is compressed. So, there is very few lateral frictions on the RI during loading. Its modulus was determined from the analysis of the loading test of the strip footing B=3 cm wide under 10×g on a polystyrene foundation 8 cm thick. For a settlement equal to 10%B, a stress equals to 70 kPa was measured. Applying the formula for an elastic medium, there comes the equivalent modulus of about 1 MPa which is representative of a soft soil.

2.2 Results and analysis

The figure 3 shows the variation of the stress under the strip footing versus its settlement at the center (y) with respect to its width (B). Figure 3.a (resp. 3.b) concerns a model with a strip footing width of 3 cm (resp. 6 cm) for a thickness H_m = 6 cm of LTP (Fig. 2).

In the case $B = H_m$ (Fig. 3.b), the admissible stress of the foundation, defined for y/B = 3%, is greater than that obtained for $B = 0.5H_m$ (Fig. 3.a): + 66% when the strip footing is above an RI, and + 128% between two RI.

For $B = H_m$, the bearing capacity of the strip footing, defined for y/B = 10%, increases by 27% if the strip footing is above the RI relative to its position between two RI.

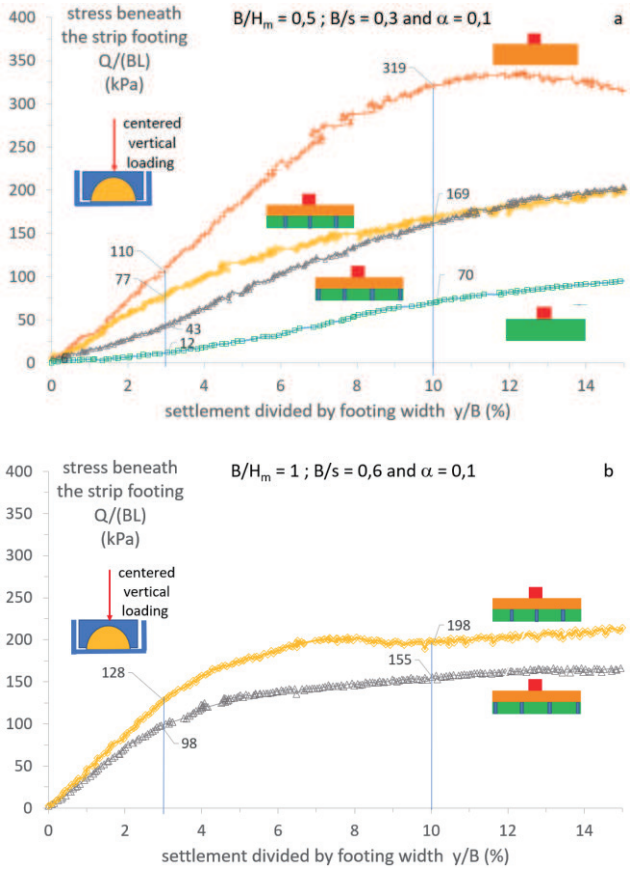

Fig. 3. Stress beneath the strip footing Q/(BL) vs the settlement (y) related to the its width (B) . a) B/Hm = 0.5, b) B/Hm = 1

For $B = 0.5H_m$, the initial stiffness of the foundation increases by 79% if the strip footing is above the RI compared to its position between two RI. But then the bearing capacities are almost equal whatever the position of the strip footing with respect to the RI. They are equal to 2.4 times the bearing capacity of the foundation on polystyrene alone and 0.5 times that of the foundation on sandy LTP alone.

2.3 Failure Mechanisms

Figure 4, in relation with Figure 3.b, relates to the quasi static loading at failure of the 6 cm wide strip footing on a 6 cm thick sand mass. The failure mechanisms are associated with the relative settlement of the strip footing equals to $y/B = 10\%$. The shear planes are identified using horizontal colored sand lines, and image analysis with the free software GeoPIV-RG (Stanier, 2016), and with a strain calculation procedure (White and Bolton, 2004).

The one drawn in Figure 4.a is an isosceles trapeze when the strip footing is between RI. The case "vertically above an RI" (Figure 4.b) both includes the former mechanism, less accentuated, and a rupture prism positioned at the head of the RI. Case b) concentrates the shear planes in the axis of the strip footing.

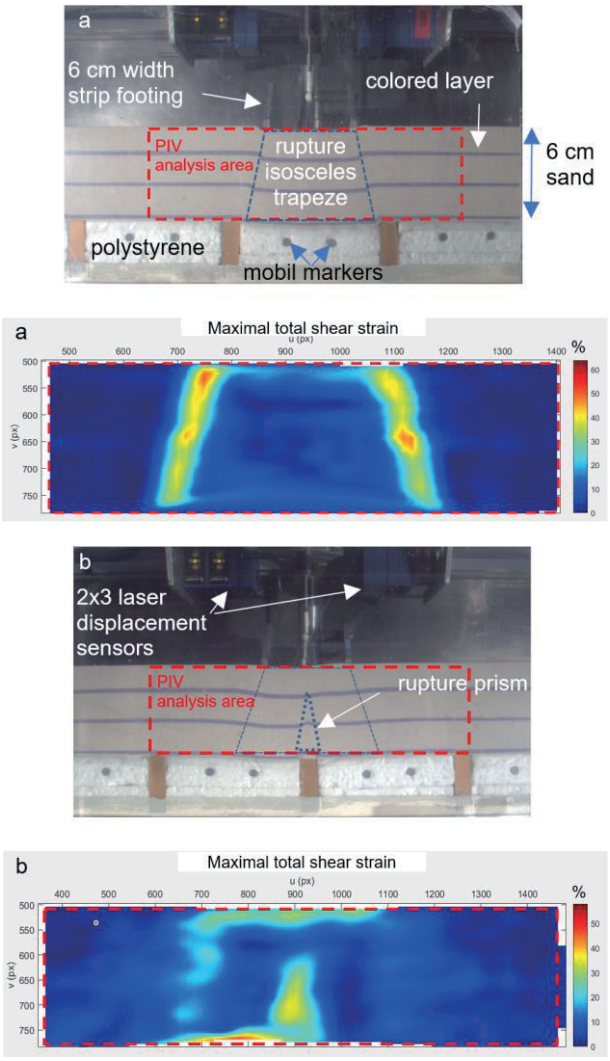

Fig. 4. Location of the maximum total shear strain in LTP at settlement equal to $0.1\times B$ such that : $B/H_m = 1$; $B/s = 0.6$ and $\alpha = 0.1$: a) between two RI ; b) above a RI

3 ROLLING LOAD

The rolling load device has also been developed in a 2D geometry. The load applied on the soil surface is deduced from the load settlement curves obtained from strip footing loading.

3.1 Design of the 2D dynamic model

A new and larger strongbox with a transparent face has been used: 80 cm long and 25 cm wide (Fig.5). The "TactArray" (PPS©) is an about 1 mm thick flexible pressure sensor pad (16×32 cells of 1 cm²), located between the soft soil and the LTP.

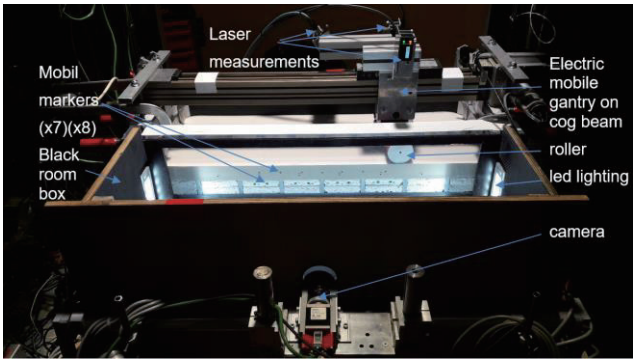

Fig. 5. The roller foundation for dynamic test behind the glass of the transparent-faced strongbox, in the centrifuge basket.

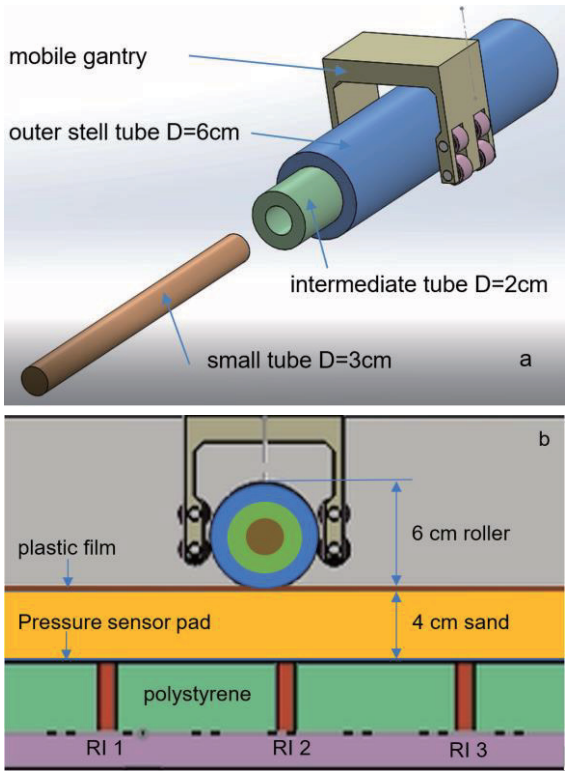

Fig. 6. Drawings of a) roller design and b) rolling gantry

The 2D rolling load consists of an outer steel tube D=6cm in outside diameter in model scale (Fig. 6.a), inside which can fit an intermediate tube D=4cm and a full tube D=2cm. Their masses are 2.9; 1.8 and 0.6 kg respectively to simulate increasing loads. The roller translation speed is 25 cm/min (Fig. 6.b). A 0.5 mm thick PVC plastic film is placed on the sand platform.

3.2 Results and analysis

The flexible pressure sensor delivers the variation of the load during the movement of the roller. On the figure 7 the evolution of the maximum vertical stress measured during rolling shows that the localization change of the rolling load induces huge variations on the maximum recorded load, especially at the vertical of each RI.

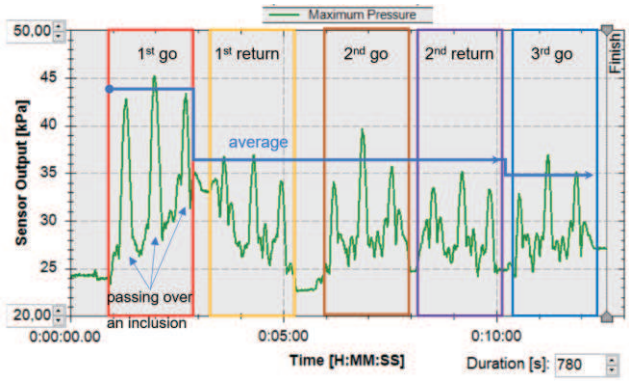

Fig. 7. Evolution of the maximum vertical stress measured by the sensor pad during the roll passages of the 2.9 kg roller.

When the 2.9 kg roller-tube (D=6cm) passes vertically over the RI, it decreases from 44 kPa, on average, on the 1st go to 36 kPa on the 1st return, and further decreases to 35 kPa on the 3rd go.

Figures 8.a and 8.b show the vertical stresses measured by the tactile pad placed on the RI and the polystyrene (Fig. 6), before rolling and after 5 round trips of the roller, respectively.

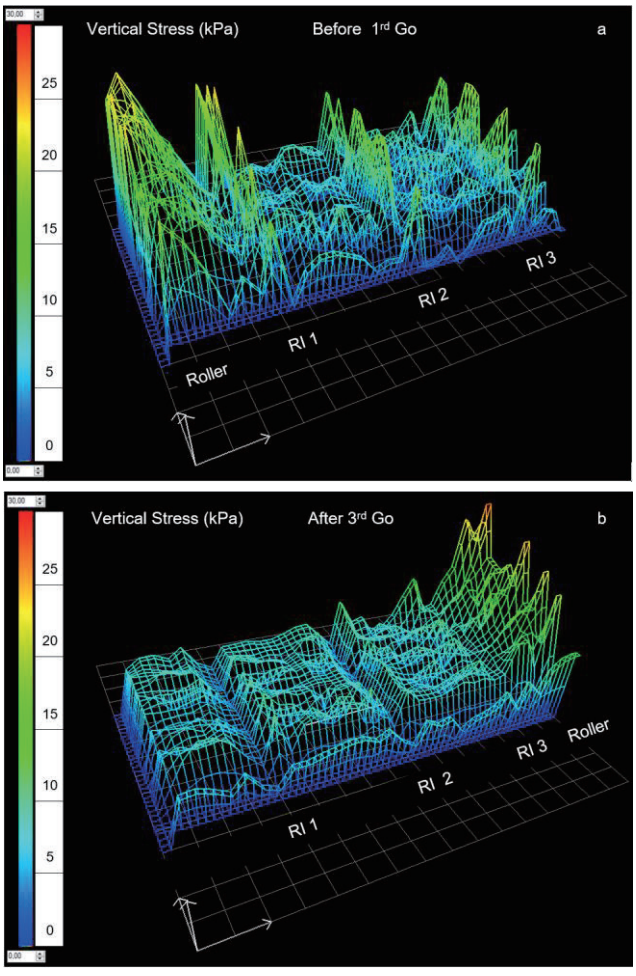

Fig. 8. Vertical stress measured by the pressure sensor pad placed on the polystyrene and the 3 RI, with 2.9 kg roller-tube D=6cm.

Before rolling, the vertical stress exerted by the roller on the polystyrene after diffusion in the sand is close to that on RI^1 (22 kPa on average). Those on RI^2 and RI^3 are lower (18 kPa on average). The average stress on the polystyrene is about 7 kPa which corresponds to the thickness of the sand above. The low stress in the polystyrene makes it possible to neglect the reinforcement that the sensor pad could provide. This stress distribution is probably due to an initial arch effect in the sandy LTP between two adjacent RI. After the 5th run, the distribution of vertical stresses between RI and polystyrene is reversed. Following the observed elastic return of the markers, the compression then the decompression of the analog soft soil with the rolling can create an inverse arch effect above the RI.

4 CONCLUSIONS

With regard to the failure mechanisms in the platform, the static tests have shown the importance of the positioning of the foundation in relation to the RI, and of its width in relation to the compressible thickness or the distance between inclusions. First simulations of 2D traffic show an evolution of the load transfer with rolling load, and a reversal effect on vertical remaining pressure above inclusions.

ACKNOWLEDGEMENTS

This work is funded by French national project ASIRI+, a cooperative research project managed by IREX with the financial support of French TE Ministry.

REFERENCES

ASIRI (French Research Project on Rigid Inclusions), 2013. Recommendations for the Design, Construction and Control of Rigid Inclusion Ground Improvements, IREX, Presses des Ponts, Paris, France. https://asiriplus.fr/.

Briançon, L., Thorel, L., Simon, B. 2020. ASIRI+: French National Research Program on soil Reinforcement with Rigid Inclusions. 4th Int. Conf. Transport. Geotech. (ICTG) Chicago, Illinois, USA Aug.30-Sept. 2. Postponed 24-27 may 2021. Proc. Adv. Transp. Geotech. IV, Lecture Notes in Civil Engng. 165, paper 462. 6p. doi.org/10.1007/978-3-030-77234-5_54

Dano, Ch., Thorel, L., Dupla, JC., Benahmed, N. 2022. Physical and mechanical properties of the NE34 Fontainebleau sand. Submitted to the Rev. Fran. Geotech. (in french).

Lukiantchuki, J.A., Oliveira, J.R.M.S., Pessin, J., Almeida, M.S.S., 2018. Centrifuge modelling of traffic simulation on a construction waste layer. Int. J. Phys. Mod. in Geotechnics 18(6): 290–300, doi.org/10.1680/jphmg.17.00012

Stanier, S., Blaber, J., Take, W., White, D. 2016. Improved image-based deformation measurement for geotechnical applications. Can. Geotech. J., 53 (5), 727-739. doi.org/10.1139/cgj-2015-0253

White, D.J., Bolton, M.D. 2004. Displacement and strain paths during plane-strain model pile installation in sand. Géotechnique, 54(6): 375-397. doi.org/10.1680/geot.2004.54.6.375